Volume 8
Number 45
7 December 2020
Pages 10213–10452

Journal of Materials Chemistry B

Materials for biology and medicine

rsc.li/materials-b

ISSN 2050-750X

ROYAL SOCIETY OF CHEMISTRY

PAPER

João Rodrigues *et al.*

New insights into the blue intrinsic fluorescence of oxidized PAMAM dendrimers considering their use as bionanomaterials

Indexed in Medline!

Journal of Materials Chemistry B

ROYAL SOCIETY OF CHEMISTRY

PAPER

View Article Online
View Journal | View Issue

Cite this: *J. Mater. Chem. B*, 2020, **8**, 10314

New insights into the blue intrinsic fluorescence of oxidized PAMAM dendrimers considering their use as bionanomaterials†

Cláudia S. Camacho, [a] Marta Urgellés,[b] Helena Tomás, [a] Fernando Lahoz [b] and João Rodrigues *[a]

Received 2nd August 2020,
Accepted 13th October 2020

DOI: 10.1039/d0tb01871f

rsc.li/materials-b

Like other bionanomaterials, dendrimers are usually labelled with fluorescent compounds in order to be optically detected within cells. However, this process can interfere with their biological properties, so it is crucial to find other solutions for their traceability. Here, the blue intrinsic fluorescence of amine-terminated poly(amidoamine) (PAMAM) dendrimers was enhanced using oxidative treatment with ammonium persulfate (APS). The effects of dendrimer generation (G3, G4, and G5) and pH on the spectroscopic behavior of both pristine and APS-treated PAMAM dendrimers were studied in aqueous solution. Overall, the results pointed out that there are at least two types of emitting electron-rich hetero-atomic sub-luminophores (HASLs) confined within the dendrimer scaffold that have very close maximum emission wavelengths and whose emission properties strongly depend on pH. The APS treatment significantly enhanced the fluorescence intensity by leading to the protonation of the interior of the dendrimer. However, fluorescence intensity was not only dependent on the number of HASLs in the dendrimer scaffold (*i.e.*, on dendrimer generation), but also on the rigidification suffered by the dendrimer due to the acidic environment (at low pH values, APS-treated G4 was indeed the most emissive species). Moreover, photoluminescence studies with lyophilized samples were also conducted, which confirmed the coexistence of more than one type of HASLs emitting in the dendrimer structure. The APS treatment affected these HASLs to a different extent. Time-resolved fluorescence experiments always showed higher average lifetimes of HASLs for APS-treated dendrimers than for pristine ones, in accordance with the fluorescence intensity results. On the other hand, the fraction and lifetimes of HASLs in APS-treated dendrimers were similar in solution and the lyophilized form. This behaviour was different for the pristine dendrimers that presented increased luminescence upon aggregation. Finally, the highly emissive oxidized dendrimers were shown not only to be much less cytotoxic and hemotoxic than pristine dendrimers but also to be detectable inside cells upon excitation with UV light.

Introduction

In the biomedical field, poly(amidoamine) (PAMAM) dendrimers have been studied as potential nanocarriers for drugs, genes, and/or bioimaging contrast agents.[1–9] Nevertheless, their application in the treatment and/or diagnosis of diseases or other medical conditions may be limited by the inherent toxicity associated with their amine termini, as well as by the lack of a strong intrinsic traceable signal that would allow their localization within cells or tissues.[10–12] To overcome these limitations, different strategies have been used, *e.g.*, decreasing or masking the amine groups at the dendrimer surface and labelling the dendrimer with fluorescent molecules, which often imply important modifications in the properties of the dendrimer and unwanted changes in their biological behavior.[13,14] For instance, the labelling of dendrimers with fluorescent probes may impact their cytotoxicity profile and modify their mechanisms of cellular internalization.[13,14]

A less known strategy relies on exploring the intrinsic fluorescence of PAMAM dendrimers,[15–19] which was recently attributed by Don Tomalia *et al.* to a non-traditional intrinsic luminescence (NTIL) phenomenon[20] that does not involve aromatic or extended π-systems but rather electron-rich hetero-atomic sub-luminophores (HASLs) confined within macromolecular architectures. This NTIL phenomenon is associated with a fluorescence emission that is often amplified by

[a] *CQM – Centro de Química da Madeira, MMRG, Universidade da Madeira, Campus da Penteada, 9000-390 Funchal, Portugal. E-mail: joaor@uma.pt*
[b] *Departamento de Física, IUdEA, Universidad de La Laguna, 38200 San Cristóbal de La Laguna, Tenerife, Spain*

† Electronic supplementary information (ESI) available. See DOI: 10.1039/d0tb01871f

the rigidification of molecular structures or by the clustering of HASLs.[20,21] Indeed, several experiments indicate that the observed weak intrinsic fluorescence of PAMAM dendrimers does not arise from their surface chemical groups but, instead, stems from chemical entities present in their internal ordered dendritic structure, like the interior amide and tertiary amine moieties that possess electron-rich heteroatoms.[15,17,20,21] In fact, NTIL emission can be observed in PAMAM dendrimers with amine, hydroxyl, or carboxylate terminal groups[15] and can be drastically enhanced through oxidative treatment, such as direct oxygen exposure[22] or by using ammonium persulfate (APS, $(NH_4)_2S_2O_8$).[16] Another important feature that should be referred to is that the fluorescence intensity shown by APS-treated dendrimers was significantly pH-dependent, increasing in acidic conditions,[23,24] as already observed for pristine dendrimers.[15]

The cumulative evidence of the existence of the NTIL phenomenon in the case of dendrimers, the interesting seminal works of Imae Toyoko *et al.*,[15,17,22,24–26] and our previous work in the application of dendrimers in the biomedical field[1,4–6,27–30] led us to study in more detail the non-intrinsic fluorescence presented by APS-treated dendrimers. Here, three generations of amine-terminated PAMAM dendrimers (G3, G4, and G5) were oxidised with APS and, after characterization *via* proton nuclear magnetic resonance (^{1}H NMR) and Fourier transformed infrared (FTIR) spectroscopies, their fluorescence properties were evaluated in solution and lyophilized forms for a better understanding of the possible mechanism underlying the observed enhanced intrinsic fluorescence. As far as we know, this is the first study of the NTIL phenomenon in APS-treated dendrimers without the interference of the solvent. Furthermore, since the ultimate purpose of these dendrimers is their potential application in the biomedical field, the effect of pH on their fluorescence intensity was studied, as well as their cytotoxicity, hemotoxicity, and visualization inside cells.

Experimental

General

Except for PAMAM dendrimers, all the reagents were used as received. Amine-terminated PAMAM dendrimers G3 (26.80 w/w%), G4 (9.99 w/w%), and G5 (19.13 w/w%) with an ethylenediamine core were acquired from Dendritech Inc. using methanol as the solvent. Before use, they were dialyzed to remove impurities. Ammonium persulfate (APS, $(NH_4)_2S_2O_8$) was supplied by PANREAC (puriss. p.a., ACS reagent, reag. Ph. Eur.), potassium dihydrogen phosphate by Merck, potassium ferricyanide by Riedel-de-Haën, potassium cyanide by Aldrich and Triton-X by Merck Millipore. Fluorescence grade pyrene was purchased from Sigma-Aldrich. The ultrapure water (UPW) used in the synthesis was obtained with a Millipore Milli-Q with a resistivity higher than 18.2 MΩ cm. All the media, solutions, and reagents used for cell culture manipulation were purchased from Life Technologies (Thermo Fischer Scientific) unless otherwise stated. The hemoglobin used in the hemotoxicity assays was from bovine blood and was purchased from Sigma-Aldrich. The healthy human blood was supplied by Hospital Dr Nélio Mendonça (SESARAM) under a collaboration between the University of Madeira/Centro de Química da Madeira and the SESARAM haematology service.

APS-treatment of PAMAM dendrimers and structural characterization

The same methodology was used for the three generations of PAMAM dendrimers. Briefly, an aqueous solution of the PAMAM dendrimer (0.2 mM) and an aqueous solution of APS (0.1 M, 20 mol equiv.) were stored in the fridge for 30 minutes. Afterward, the APS aqueous solution was dropwise added into the PAMAM dendrimer solution. The mixture was allowed to react under magnetic stirring at room temperature for three days. The solution was then lyophilized, always leading to a pale-yellow viscous liquid.

Proton nuclear magnetic resonance (^{1}H-NMR) spectra were recorded with a Bruker UltraShield™ 400 Plus Ultra Long Hold NMR spectrometer at room temperature using D_2O as the solvent. Chemical shifts (δ) were reported in ppm and referenced relatively to the residual proton of the deuterated solvent. The Fourier transformed infrared (FTIR) spectra of lyophilized samples were recorded in KBr pellets using a PerkinElmer Spectrum Two spectrometer in the 4000–400 cm^{-1} range.

UV-Vis spectroscopy and photoluminescence studies

The obtained pale-yellow viscous liquids containing the oxidized PAMAM dendrimers were dissolved in ultrapure water (UPW), and irradiated using UV light (366 nm) to collect the images shown in Fig. 3 and Fig. S6 (ESI†).

UV-Vis spectroscopy studies in solution were performed in the range of 200–600 nm using a PerkinElmer Lambda 25 UV-Vis spectrometer. Photoluminescence (PL) studies in solution were conducted using a PerkinElmer LS 55 fluorescence spectrometer in the range of 300–700 nm using a 10 mm-path quartz cell and excitation and emission slit widths set at 12 nm and 5 nm, respectively. Emission spectra were recorded using an excitation wavelength of 380 nm (λ_{ex}), and excitation spectra were recorded, setting the emission wavelength at 450 nm (λ_{em}). Studies at different pH values were conducted in a universal buffer solution (6 g of citric acid, 3.9 g of monopotassium phosphate, 1.8 g of boric acid, and 5.3 g of diethyl-barbituric acid in 1 L of UPW) by adjusting the pH of the solution using HCl or NaOH 1 M solutions.

Relative quantum yields for the APS-treated PAMAM dendrimers were calculated using the single point method.[31] The following equation was used:

$$Q = Q_R \frac{I}{I_R} \frac{OD_R}{OD} \frac{n^2}{n_R{}^2} \quad (1)$$

where Q is the fluorescence quantum yield, I is the integrated fluorescence intensity, n is the refractive index of the solvent (water), and OD is the optical density. The subscript R denotes the value for the reference, that is, for the fluorophore of known

quantum yield. The reference fluorophore used was pyrene in cyclohexane, which presents a quantum yield of 32% (λ_{ex} = 317 nm).[32] The concentration used for pyrene and APS-treated PAMAM dendrimers was 1×10^{-5} M. The absorbance value used was the value at a wavelength of 380 nm (the excitation wavelength used in fluorescence emission studies).

The diffuse reflectance of the lyophilized material was measured in the 250–500 nm spectral range using an Agilent Cary 5000 spectrophotometer equipped with an integrated sphere. The photoluminescence (PL) spectra of the lyophilized material were recorded using a 405 nm picosecond pulsed diode laser (Edinburgh Instruments EPL-405) with a typical pulse width of 80 ps. The emission spectra and fluorescence decays were recorded using a fluorescence spectrometer with a single photon counting multichannel plate photomultiplier and dedicated acquisition software (Edinburgh Instruments LifeSpec II and F900 software). Fitting of the fluorescence decays to multi-exponential decay functions was performed using the reconvolution of the instrumental response function (IRF) of the equipment (Edinburgh Instruments FAST software).

Cytotoxicity evaluation

CAL-72, a human osteosarcoma cell line, and NIH 3T3, a mouse fibroblast cell line, were purchased from DSMZ. Both cell lines were cultured in Dulbecco's Modified Eagle's medium (DMEM) containing 1% (v/v) antibiotic–antimycotic 100× solution (AA, containing penicillin, streptomycin, and amphotericin B) and 10% (v/v) foetal bovine serum (FBS), at 37 °C, in a humidified atmosphere with 5% carbon dioxide. For CAL-72 cells, the medium was also supplemented with 1% (v/v) insulin–transferrin–selenium 100× solution (ITS) and 1% (v/v) L-glutamine solution (100×).

For cell culture experiments, both cell lines were cultured in 48-well plates at a seeding density of 10×10^3 cells per well. After 24 h, the medium was replaced with a fresh one, and the cells were incubated with the APS-treated PAMAM dendrimers (G3, G4, and G5) prepared in PBS buffer (pH 7.4) within the concentration range of 0.25–20 μM. Pristine PAMAM dendrimer solutions were used as controls.

The cytotoxicity of APS-treated dendrimers was indirectly evaluated by measuring the metabolic activity of cells through the resazurin reduction assay. After a 48 h incubation period, the cell culture medium was replaced with a new medium containing resazurin at a concentration of 0.1 mg ml^{-1}, and the cells were further incubated for 3 h at 37 °C. Afterwards, aliquots of cell medium were transferred to the wells of 96-well opaque plates, and the fluorescence of resorufin was measured using a PerkinElmer VICTOR$^{3™}$ microplate reader (λ_{ex} = 530 nm, λ_{em} = 590 nm). The metabolic activity is presented as a percentage of the control (cells cultured in the absence of dendrimers). The results are expressed as the mean ± SD of two independent experiments with three replicates of each.

Hemotoxicity evaluation

Hemotoxicity assays were carried out using fresh and healthy human blood. For the determination of the total hemoglobin concentration in the original blood, a 250-fold dilution of blood was prepared in cyanmethemoglobin reagent, which is also called C reagent (20 μl of blood in 5 ml of C reagent). The C reagent (50 mg potassium ferricyanide, 12.5 mg potassium cyanide, and 35 mg potassium dihydrogen phosphate in 250 ml of distilled water) was prepared in an amber bottle with 250 μl Triton-X, and its pH was adjusted to 7.4. A standard curve for hemoglobin was then established using hemoglobin from bovine blood (ESI,† Fig. S1). For that purpose, a stock solution of the protein (1.5 mg ml^{-1}) was prepared using C reagent as the solvent. From this stock solution, serial dilutions were performed to obtain standards of known concentration (0.20, 0.37, 0.54, 0.7, 0.88, 1.05, 1.22 and 1.39 mg ml^{-1}) and the absorbance was measured at 550 nm. The C reagent was used as the blank. The purity of the commercial hemoglobin was very good, as assessed by the ratio of absorbance values at 550 nm and 405 nm. The absorbance of the diluted solution of blood was then measured, and its concentration was determined.

For the hemotoxicity evaluation of the oxidized dendrimers, the compounds were dissolved in distilled water (30 μM) and diluted to concentrations of 0.1, 1, and 5 μM using PBS solution (Mg^{2+}/Ca^{2+} free). Then, 1 ml of a 10% (v/v) blood solution was prepared in PBS (Mg^{2+}/Ca^{2+} free), and 10 μl of this solution was placed into microcentrifuge tubes, one for each compound and concentration to test, including a positive and a negative control. Then, the blood solution was added to 70 μl of each sample and 70 μl of water or PBS for the positive and negative controls, respectively, and incubated for 3 h at 37 °C. Following the incubation period, the mixture was centrifuged at 3800 rpm for 10 min. Then, 40 μl of each supernatant was transferred to 96 well plates, and 160 μl of the C reagent was added. The absorbance values of the supernatants were measured at 550 nm in the microplate reader, and the prepared standard curve was applied to determine their hemoglobin concentrations. The same procedure was performed for the pristine PAMAM dendrimers. Taking into account the dilutions made throughout the assay, the percentage of hemolysis was then calculated for each situation from the ratio between the hemoglobin concentration in the sample's supernatant and the total value that was initially present multiplied by 100. The results are presented as mean ± SD for three independent assays.

Fluorescence microscopy studies

The human bone osteosarcoma epithelial (U2OS) cell line was cultured in Dulbecco's modified Eagle's medium (DMEM, high glucose, GlutaMAX) with 10% (v/v) FBS and 1% (v/v) penicillin–streptomycin solution under standard cell culture conditions. Cells were grown at 37 °C in a 5% carbon dioxide incubator until reaching 50–80% confluence before being used in the experiments. Cells were then incubated with the APS-treated PAMAM dendrimer G4 for 24 h at 2 μM. Cell culture images were collected using a Cell Observer fluorescence microscope (Zeiss) with a 40× objective, equipped with a black and white photographic camera (Zeiss Axiocam 503 mono) and Zen software for image acquisition.

Results and discussion

Structural characterization of dendrimers

Three different generations of PAMAM dendrimers with amine terminal groups (G3, G4, and G5) were oxidized using ammonium persulfate and characterized *via* ^{1}H-NMR. Comparing each spectrum obtained with the corresponding spectrum of the pristine dendrimer, it is possible to observe a downfield shift of the main NMR signals for the APS-treated PAMAM dendrimers (see Fig. S2–S4 in the ESI,† as well as Table S1). In fact, it is known that, beyond hydrogen peroxide that decomposes originating oxygen, APS hydrolysis also gives rise to other chemical species in solution, such as permonosulfuric acid, peroxymonosulfate, and sulfuric acid.[33] Although the effect of APS on PAMAM dendrimers is still not very well understood, there is evidence that these species confer an acidic environment and cause the protonation of amine groups of the dendrimer.[23] Our ^{1}H-NMR results support this finding since the protonated amines will act as electron-withdrawing agents and cause the downfield shift of the signals arising from the protons in the vicinity of both the primary and the tertiary amines. Imae *et al.* also reported the downfield shift of the signal of the methylene protons adjacent to the peripheral amines[24] for APS-treated dendrimers. In our case, a deshielding of the protons surrounding the tertiary amines was observed too. Additionally, the strength of hydrogen bonds between the oxygen in the –C═O moiety and the proton in the –NH moiety increases under acidic conditions, which further contributes to proton deshielding.[23] This behaviour was similar for all the tested dendrimer generations.

The amine-terminated PAMAM dendrimers and APS-treated ones were also studied *via* FT-IR spectroscopy (ESI,† Fig. S5A–C). The spectra of all three generations of pristine dendrimers show the characteristic bands of the amide group (–CONH–).[23,34–36] The amide A band due to N–H stretching vibration (very sensitive to the strength of hydrogen bonds) appears at 3200–3300 cm^{-1}. Amide B, an overtone of amide II, can be seen around 3080 cm^{-1}. Amide I, an intense band mainly associated with the C═O stretching vibration, arises near 1635 cm^{-1}. The amide II band, mainly resulting from in-plane C–N–H bending and C–N stretching, is also evident near 1550 cm^{-1}. Other amide-associated bands (from III to VI) are also present in the spectra, although they are more difficult to analyse. Methylene group bands appear at around 2945 cm^{-1} (asymmetric C–H methylene stretching), 2850 cm^{-1} (symmetric C–H methylene stretching), and 1435–1465 cm^{-1} (H–C–H scissoring and asymmetric deformations). Shoulders near 1060 cm^{-1} reflect the –C–N stretching band for tertiary amines. Two bands from skeletal C–C stretching at 1130–1150 cm^{-1} can also be seen in the spectra. The primary amines present at the surface of dendrimers should absorb radiation in the region of 3250–3400 cm^{-1} (due to two modes of N–H stretching), and the corresponding bands appear overlapped with the amide A band and, possibly, with bands related with the presence of traces of water.

The APS treatment has a strong impact on the FTIR spectra of dendrimers, which includes the effect of the generated acidic environment that results in amine protonation, as well as the presence of sulfur-containing chemical species produced during APS hydrolysis. Indeed, Saravanan and Abe[23] showed through XPS analysis that SO_4^{2-} (sulfur VI) and $S_2O_3^{2-}$/S^{2-} (sulfur II) ions are present in PAMAM dendrimers with hydroxyl termini after APS treatment. These are stable ions that end up interacting with the protonated amine groups. Our results obtained with PAMAM dendrimers containing amine termini are generally in line with this work. A broad band is evident above 2400 cm^{-1} that results from the overlap of several signals, including those from protonated amines (ammonium groups). Another broad band appears around 1105 cm^{-1} due to the overlapping of the –C–N stretching band of tertiary amines, the bands from skeletal C–C stretching, and also the bands related to the presence of sulfur species (namely SO_4^{2-} that usually presents a band corresponding to asymmetric stretching around 1090 cm^{-1}). After the oxidative treatment, a sharp band near 615 cm^{-1} was also observed, which can be assigned to certain modes of vibration of the amide group (like the amide VI band) or, most probably, to the presence of SO_4^{2-} since this ion shows signals near this frequency caused by out-of-plane bending vibration.[37] The amide I band, which is highly sensitive to small variations in hydrogen bonding, shifted toward higher frequencies (from around 1635 cm^{-1} to 1660 cm^{-1}), whereas the signals of methylene groups became weaker. These findings are consistent with a more acidic environment conferred by APS treatment.

UV-Vis spectroscopy studies

Fig. 1 shows the absorbance spectra of pristine and APS-treated PAMAM dendrimers (generations 3, 4, and 5) in aqueous solution. After the oxidative treatment, the slight shoulder that appeared around 280–290 nm in the pristine dendrimers (see Fig. 1d that shows the spectra using an expanded scale) became much more intense (a band is clearly seen). Crooks *et al.*[38] performed studies with pristine amine- and hydroxyl-terminated PAMAM dendrimers and concluded that this band is related to radiation absorption by the tertiary amines present in the interior of the dendritic structure. They showed that the intensity of this band increased with the increasing pH and that the process was reversible. Our results with pristine dendrimers also reveal the presence of this band, which increases in intensity with dendrimer generation, that is, it increases with the number of tertiary amines present in the dendrimer scaffold. However, we show that the same band appears in the spectra of APS-treated PAMAM dendrimers with intensity values that are several orders of magnitude higher than those observed in pristine dendrimers (Fig. 1e) and despite the protonation of tertiary amines in the interior of the dendrimers. In our experiments, both the pristine and the oxidized dendrimers display an absorbance band with a maximum at 280–290 nm, in contrast to the observations made by Abe *et al.* that reported a red-shift of this band to 360 nm after APS treatment of dendrimers with hydroxyl surface groups.[23]

It should, however, be noted that the absorption spectra of pristine dendrimers reveal the presence of at least two more bands in the ranges 300–400 nm and 400–500 nm

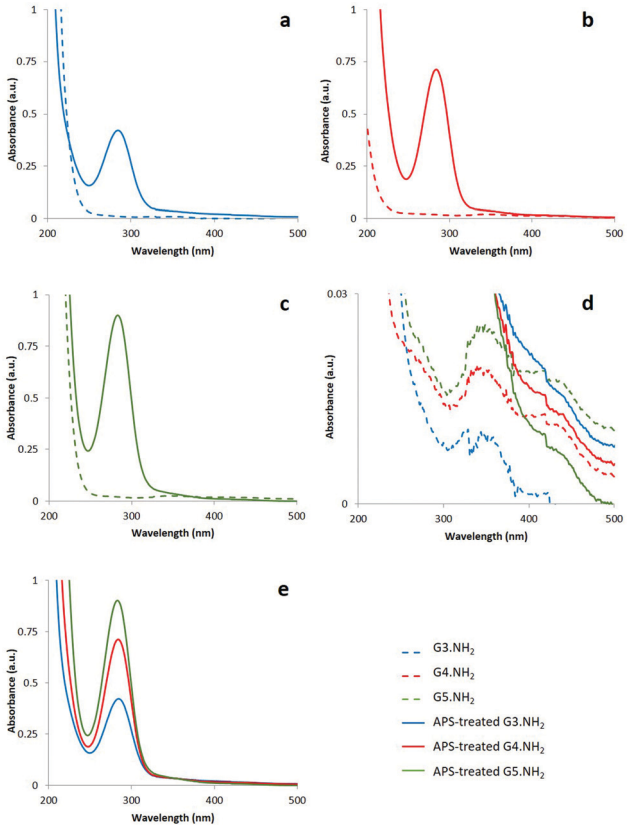

Fig. 1 Absorption spectra of pristine and APS-treated PAMAM dendrimers for generations (a) G3, (b) G4, and (c) G5. (d) Absorption spectra are shown on an expanded scale. (e) Comparison of absorption spectra among the three generations of APS-treated PAMAM dendrimers. Spectra were recorded at a concentration of 1×10^{-5} M in ultrapure water.

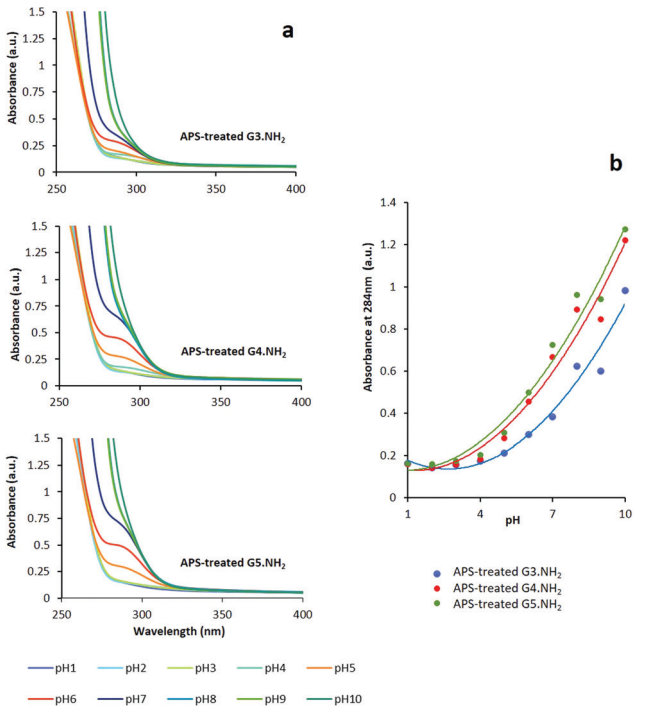

Fig. 2 (a) Absorption spectra of APS-treated PAMAM dendrimers recorded in a buffer solution at a concentration of 1×10^{-7} M and different pH values. (b) Comparison of absorbance values at 284 nm among the three generations of APS-treated PAMAM dendrimers.

(although having a very low intensity). These bands may also exist in the spectra of APS-treated PAMAM dendrimers which were camouflaged by the 280–290 nm band of higher intensity.

The effect of pH on the absorbance of generations 3, 4, and 5 of APS-treated PAMAM dendrimers was then studied by recording absorption spectra in a buffer having the same chemical composition but adjusted to different pH values (Fig. 2). In general, the intensity of the band at 280–290 nm increases with dendrimer generation and with the pH value. When the absorbance intensity at 284 nm is plotted against pH, an increase after pH $\approx$ 3 can be clearly observed. At very low pH, for high levels of dendrimer protonation, the absorbance values are identical for all generations. As the pH increases, the level of dendrimer protonation is different for each generation, and absorbance values become distinct among them. The absorbance is higher for generation 5, followed by generation 4 and generation 3. Indeed, our results show that the dependency of absorbance at 284 nm on the solution pH for APS-treated PAMAM dendrimers is identical to what was reported by Crooks *et al.* for pristine PAMAM dendrimers[38] with both amine or hydroxyl surface termini. Like Crooks *et al.*, we obtained opposite results to Fu *et al.*[39] who conducted UV-Vis experiments with sectorial PAMAM dendrimers containing amine surface groups.

Photoluminescence studies in solution

The pale-yellow viscous liquids obtained after the synthesis of the APS-treated dendrimers were dissolved in UPW at a concentration of 1×10^{-3} M. After irradiation under UV light at 366 nm, blue luminescence could be observed. Fig. 3 qualitatively shows the extent of fluorescence intensity for G3, G4, and G5 dendrimer aqueous solutions prepared at the same concentration (G3 > G4 > G5). An evident difference in terms of luminescence was clearly seen among the generations (see also the ESI,† Fig. S6).

Fig. 4 shows the excitation and emission fluorescence spectra of pristine and APS-treated PAMAM dendrimers (generations 3, 4, and 5) in aqueous solution. After excitation at 380 nm, an emission band can be observed for both cases in the blue spectral region with intensity values being much higher for the APS-treated dendrimers than those for the

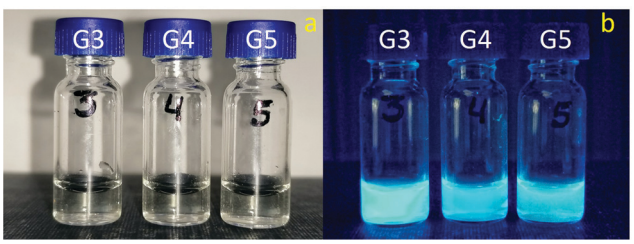

Fig. 3 APS-treated PAMAM dendrimers (G3–G5) with a concentration of 1×10^{-3} M in ultrapure water in the absence (a) and presence of UV irradiation (366 nm) (b).

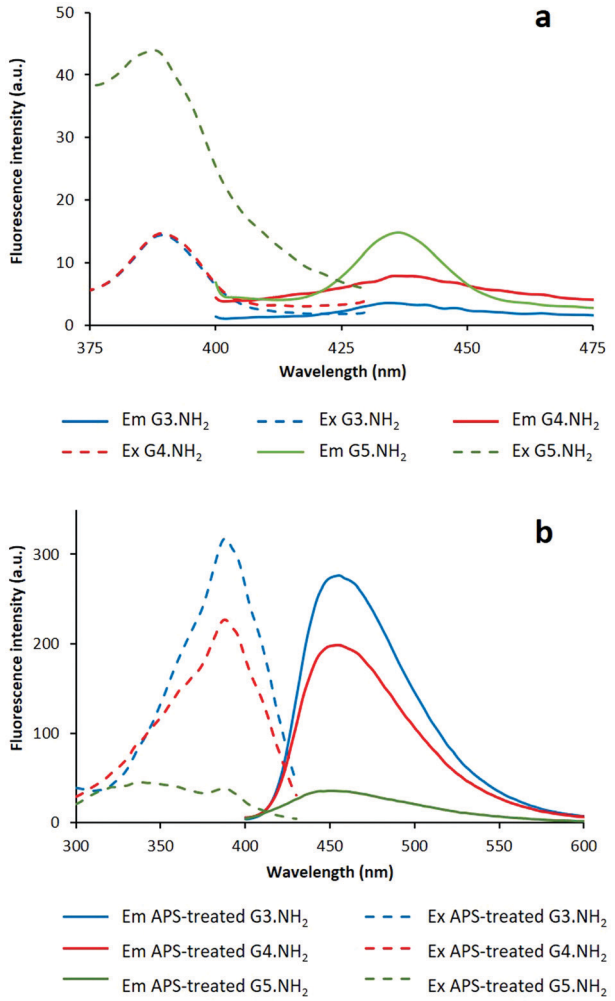

Fig. 4 Emission (λ_{ex} = 380 nm) and excitation (λ_{em} = 450 nm) spectra of pristine (a) and APS-treated (b) PAMAM dendrimers. Spectra were recorded at a concentration of 1×10^{-5} M in ultrapure water.

corresponding pristine ones. Although the excitation spectra revealed another band at *ca.* 250 nm (ESI,† Fig. S7), fluorescence emission intensities were higher when 380 nm was used as the excitation wavelength. Interestingly, the excitation spectra show a very weak signal at *ca.* 280–290 nm corresponding to the dominant absorption band in the UV-vis spectra. So, the blue fluorescence emitted by the APS-treated dendrimers resulted from excitation in the range of 300–425 nm (as mentioned above, radiation absorption in this wavelength range is clearly observable in the UV-vis spectra of pristine dendrimers and is probably hidden by the intense 280–290 nm absorption band in the UV-vis spectra of APS-treated dendrimers).

The maximum wavelength of fluorescence in the emission spectra displayed a red-shift from around 437 nm in the spectra of pristine dendrimers to about 450 nm in the spectra of APS-treated dendrimers. Moreover, whereas the fluorescence intensity increased with generation in pristine dendrimers (Fig. 4a), it displayed an opposite trend in the case of APS-treated dendrimers (Fig. 4b). However, it must be noticed that these spectra were all recorded in water. In fact, we could later conclude that the emission of fluorescence by APS-treated dendrimers was strongly pH-dependent, a characteristic already reported for pristine PAMAM dendrimers.[15] When spectra were recorded in buffer solutions of different pH values (Fig. 5a), it was evident that the fluorescence intensity was much higher at low pH (Fig. 5b), highlighting the role of protonation in the fluorescence behaviour of APS-treated dendrimers. For all three generations of APS-treated dendrimers, the fluorescence intensity significantly increased below pH 7, had maximum values in the 3–5 pH range, and then decreased again at very low pH. Unexpectedly, at a pH lower than 7, generation 4 APS-treated PAMAM dendrimers were the most emissive, followed by generation 5 and then by generation 3. Indeed, the increase in fluorescence intensity when lowering the pH was much more marked for the highest generations than for generation 3. Another observation from these studies is that the maximum wavelength of fluorescence emission increases with an increase in the concentration of H^+ in solution (pH decrease), as depicted in Fig. 5c. Moreover, there was a pronounced jump in this value when decreasing the pH from 7–8 to 6, similarly to what was observed with the fluorescence intensity. Interestingly, the pK_a of the tertiary amines (around 6.3[38]) was included within this interval of pH. In the

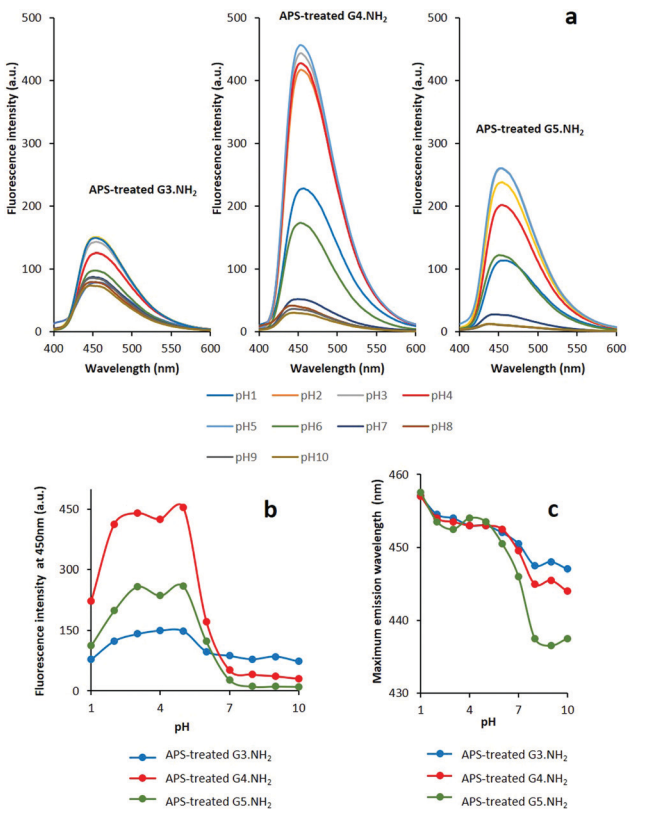

Fig. 5 (a) Emission (λ_{ex} = 380 nm) spectra of generation 3, 4 and 5 APS-treated PAMAM dendrimers recorded in a buffer solution at a concentration of 1×10^{-6} M and different pH values. (b) Effect of pH on fluorescence intensity at 450 nm. (c) Effect of pH on the maximum wavelength of fluorescence emission.

range of pH 2–6 (low emission zone), the maximum wavelength of fluorescence emission remained constant.

These results show that the protonation of the tertiary amine groups in APS-treated dendrimers strongly affects fluorescence emission. Indeed, the protonation of the tertiary amine groups in the interior of the dendritic structure has been associated with molecular conformational and polarity changes.[40] Moreover, as recognized by other researchers, it will result in high internal repulsion forces among dendrimer branches, thus making the overall structure more rigid.[15,23] Rigidity is also promoted by the increase in the strength of the hydrogen bonds that occurs in an acidic environment.[15,41]

In summary, our photoluminescence studies performed with the APS-treated dendrimers in solution support the ideas underlying the NTIL phenomenon described by Tomalia *et al.*[20] Fluorescence intensity not only depends on the number of HASLs confined in the dendrimer scaffold (that is, on dendrimer generation) but is also enhanced by scaffold rigidification that occurs as a consequence of APS treatment. The results obtained for the three different generations of dendrimers in Fig. 5 should then be a compromise between these two parameters. For example, although APS-treated G4 dendrimers have a lower number of HASLs than their G5 counterparts, they should adopt a more rigid conformation under low pH conditions that promote fluorescence emission. Also, one should notice that, independently of the generation, the emission spectra were not symmetrical. Regarding this observation, there are three possibilities: different HASLs inside the dendrimer structure may exist emitting at different wavelengths; the same HASLs may exist in multiple chemical environments (at least more than one) that modulate fluorescence emission; and, finally, both situations may coexist. In fact, a study using quantum chemical theory methods concluded that there are two potential emitting moieties in pristine PAMAM dendrimers: the imidic acid resonance structure from the amide, the formation of which is promoted at low pH values, and the tertiary ammonium groups formed upon protonation of tertiary amines.[35] Calculations assuming the dendrimers in the gas phase showed that these species could theoretically emit fluorescence at 308 nm (the imidic acid) and 370 nm (the tertiary ammonium group).[35] Also, a recent work devoted to the study of fluorescence quenching in pristine PAMAM dendrimers points out that there are two distinct fluorescent moieties in their structure with the emission maxima separated by 40 nm.[42] It is therefore reasonable to assume that the amide and tertiary amine groups that exist in the dendrimer scaffold constitute two distinct HASLs with photoluminescence properties that are dependent on the pH environment which is in turn strongly affected by the APS treatment. However, it seems that the APS treatment does not exert its effect to the same extent in both HASLs as it causes a red shift in the maximum wavelength of fluorescence. In other words, it increases the number of HASLs that emit at a higher wavelength, which, according to the literature,[35] should be the tertiary ammonium groups.

The quantum yield of a fluorophore is an important parameter as it informs about the ratio of photons emitted to photons absorbed; that is, it is a measure of the efficiency of the process. Quantum yields were determined for PAMAM dendrimers after the oxidative treatment using pyrene as a reference. Generation 3 APS-treated PAMAM dendrimers were the ones with the highest quantum yield (75%), followed by generation 4 (63%) and generation 5 (15%). Interestingly, Klajnert-Maculewicz *et al.* also found a decrease in quantum yield with an increase in the generation of pyrrolidone-terminated PAMAM dendrimers.[43]

Photoluminescence studies in lyophilized samples

The absorption spectra of the dendrimers in the lyophilized form were obtained from diffuse reflectance measurements. The results are shown in Fig. 6. The absorption spectrum of the G3 pristine PAMAM dendrimers is formed by a band centred at about 280 nm, which is in line with what was observed in the previous UV-vis spectroscopy experiments performed in solution. A shoulder appears at the low energy side of the absorption band for pristine G4 and G5 dendrimers, which evidences the effect of the additional shells of the dendrimer on the absorption centres as the generation increases (in fact, very low-intensity absorbance bands in the ranges of 300–400 nm and 400–500 nm were also present in the UV-vis spectra of pristine dendrimers in solution; see Fig. 1d).

Also, here the APS treatment has a substantial impact on the absorption spectrum. An intense absorption band appears in the 300–400 nm spectral range, which overlaps the one centered at 280 nm. As mentioned previously, the corresponding absorption bands may be present in the UV-vis spectra of APS-treated dendrimers recorded in solution although camouflaged by the dominant 280–290 nm band (Fig. 1d). However, experiments with the dendrimers in the lyophilized form clearly evidence the existence of absorption at wavelengths above 300 nm.

The emission spectra of the APS-treated and pristine G3, G4, and G5 PAMAM dendrimers were recorded under excitation at

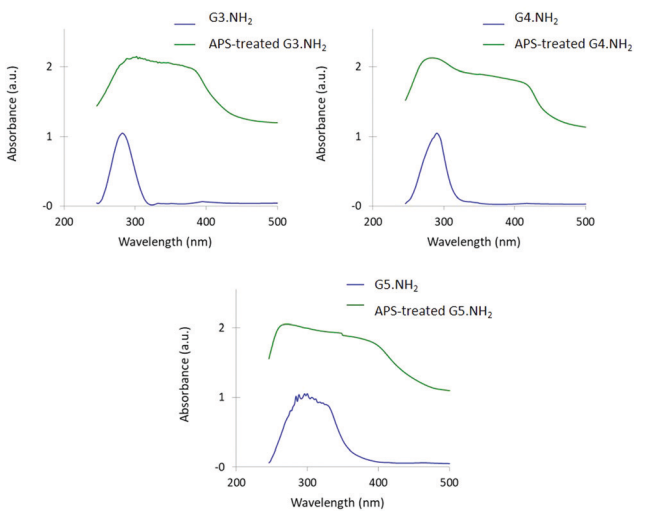

Fig. 6 Normalized absorption spectra of pristine PAMAM dendrimers and APS-treated PAMAM dendrimers (G3, G4, and G5) in the lyophilized form.

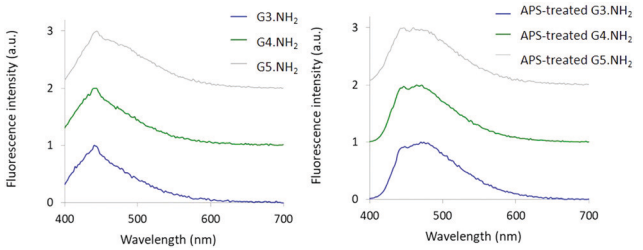

Fig. 7 Normalized emission spectra of pristine PAMAM dendrimers and APS-treated PAMAM dendrimers (G3, G4, and G5) in the lyophilized form (λ_{ex} = 380 nm).

405 nm (Fig. 7). In the case of the pristine dendrimers, the emission is formed by two overlapping bands. One is centred at about 445 nm and the other around 475–480 nm. The relative intensity of the second band increases as the generation of the PAMAM dendrimer is higher. The APS-treated dendrimers present emission spectra formed by the same two overlapping bands, but the relative weight of the second band is more significant. These results are compatible with the hypothesis of the coexistence of more than one type of HASLs emitting in the dendrimer structure and that the APS treatment does not affect the fluorescence intensity of both in the same manner.

A quantitative comparison of the emission intensities in the lyophilized samples remains challenging since differences in the quantity and compactness of the sample have a direct influence on the results. However, one may qualitatively say that emission intensities of the same order of magnitude were obtained in this case for the APS-treated and pristine PAMAM dendrimers. This result is quite different from the one observed in the aqueous solution where the APS-treated dendrimers showed emission intensities several orders of magnitude higher than the pristine ones (Fig. 4). To investigate this finding, time-resolved fluorescence measurements were conducted in G3, G4, and G5 pristine and APS-treated PAMAM dendrimers.

Time-resolved fluorescence experiments

The decays of the fluorescence of G3, G4, and G5 pristine and APS-treated PAMAM dendrimers were recorded at the maximum of the emission bands when the excitation was tuned at 405 nm. Both lyophilized samples and water solutions at a concentration of 2×10^{-5} M were tested and compared (Fig. 8). Based on the previous experiments and assuming the existence of two HASLs in the dendrimer structure, the decay curves were fitted to a double exponential decay equation:

$$I(t) = A_1 e^{-t/\tau_1} + A_2 e^{-t/\tau_2} \quad (2)$$

where τ_1 and τ_2 are the decay constants of the fast and slow components, respectively, and A_1 and A_2 represent the pre-exponential factors that should correspond to the fraction of each HASL. An average lifetime (τ_{av}) is then defined using the equation:[31]

$$\langle \tau_{av} \rangle = \frac{A_1\tau_1^2 + A_2\tau_2^2}{A_1\tau_1 + A_2\tau_2} \quad (3)$$

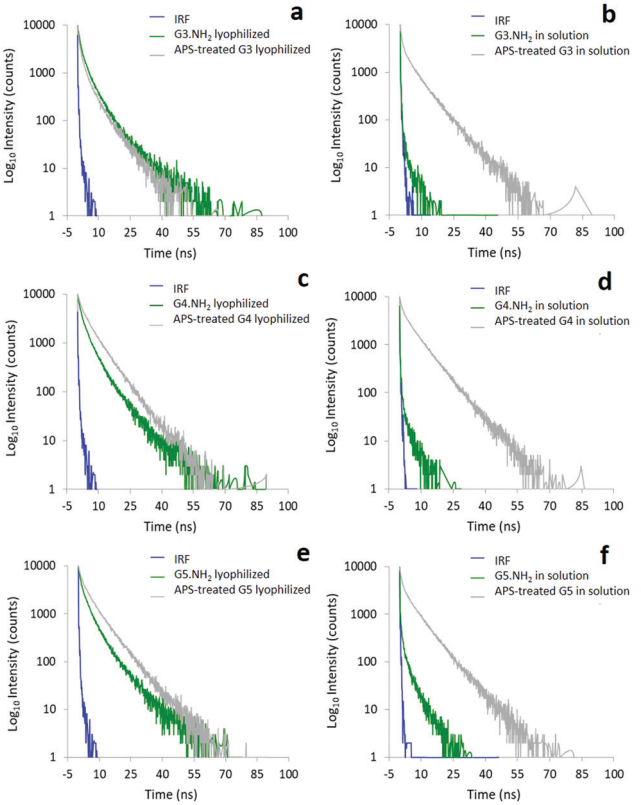

Fig. 8 Decay of the fluorescence of pristine and APS-treated (a) G3, (b) G4, and (c) G5 PAMAM dendrimers in lyophilized form and (d) G3, (e) G4, and (f) G5 PAMAM dendrimers in aqueous solution.

The decay curves were fitted to eqn (2), taking into account the reconvolution of the IRF of the experimental setup. Table 1 shows the pre-exponential factors, τ_1 and τ_2, and the average lifetime obtained from the fitting procedure.

In solution and for the three dendrimer generations, the decay of the APS-treated dendrimers is clearly longer than those of the non-treated precursors, that is, corresponds to higher average lifetimes. When analysing the pre-exponential factors, one can see that there is a predominance (99–100%) of very fast emitting components (0.01–0.02 ns) in the pristine dendrimers, whereas increased higher average lifetimes (4.92–5.91 ns) are observed in their APS treated counterparts. The average lifetimes in APS-treated dendrimers result from a combination of fast emitting components (0.70–1.12 ns) with slow emitting ones (7.05–7.50 ns) in a proportion of 69–82% and 18–31%, respectively. These lifetime results are in agreement with the higher emission intensities observed in the APS-treated dendrimers in aqueous solution as compared to the pristine ones (Fig. 4). Assuming that the HASLs in dendrimers are the imidic acid and the tertiary ammonium groups and based on the results and data from the literature,[35] we propose that tertiary ammonium groups are HASLs with longer fluorescence lifetimes.

In the lyophilized form, except for G3 PAMAM dendrimers, APS-treated dendrimers still show higher average lifetimes than

Table 1 Fitting parameters and the average lifetime of G3, G4, and G5 pristine and APS-treated PAMAM dendrimers in aqueous solution and in lyophilized form

	A_1	τ_1 (ns)	A_2	τ_2 (ns)	τ_{av} (ns)
Lyophilized					
APS-treated G3	0.96	0.83	0.04	5.15	1.78
APS-treated G4	0.64	1.52	0.36	6.68	5.19
APS-treated G5	0.70	1.47	0.30	6.99	5.16
G3·NH_2	0.89	1.13	0.11	5.30	2.68
G4·NH_2	0.82	1.38	0.18	5.58	3.34
G5·NH_2	0.86	1.17	0.14	5.48	3.04
Solution					
APS-treated G3	0.81	0.70	0.19	7.05	5.15
APS-treated G4	0.69	1.12	0.31	7.50	5.91
APS-treated G5	0.82	0.93	0.18	7.27	4.92
G3·NH_2	0.9999	0.01	0.0001	3.16	0.01
G4·NH_2	0.9999	0.01	0.0001	2.68	0.01
G5·NH_2	0.999	0.02	0.001	2.8	0.04

pristine ones ($\approx$5 ns *vs.* $\approx$3 ns), although belonging to the same order of magnitude. This explains the observed qualitatively similar fluorescence intensities for both cases. In APS-treated dendrimers, the characteristics of both slow and fast emitting HASLs are very similar when comparing the results of the fitting parameters obtained for lyophilized and solution samples.

Nevertheless, the most notable finding in these studies is when the lyophilized samples of pristine dendrimers are compared with the corresponding solution samples. Much longer average lifetimes (2.68–3.34 ns) are observed in the lyophilized form than those in solution (0.01–0.04 ns). This can be explained in light of the NTIL theory that states that NTIL emissions can be enhanced by HASL aggregation.[20] This property is also observable in many other systems and gives rise to higher fluorescence intensities.[20,44] The mechanism of aggregation-induced emission is very well elucidated by Ben Tang *et al.* in an excellent review[44] and may be applied here for the pristine dendrimers. In solution, the dynamic intramolecular motions in dendrimers extinguish their excited-state energy, whereas, in the lyophilized/aggregated form, the restriction of these motions allows the excited state energy to be released *via* a radiative pathway. This same mechanism can explain why scaffold rigidification can also result in an increase in fluorescence intensity. Most likely, this phenomenon does not occur with APS-treated dendrimers since they are protonated, and the molecules are less aggregated in the lyophilized sample because of repulsion forces existing among them.

In vitro cytotoxicity studies

For the application of dendrimers as bionanomaterials, it is very important to assure that they will not compromise cell viability. In fact, regarding PAMAM dendrimers, it is well known that their toxicity behaviour is dependent on the generation, concentration, and type of terminal groups. PAMAM dendrimers with amine termini can be particularly toxic due to their high positive surface charge under physiological conditions.[10,11] As such, we aimed to investigate the cytotoxicity of the APS-treated PAMAM dendrimers and compare it with that of the pristine dendrimers.

The cytotoxicity of dendrimers was then evaluated *in vitro* using NIH 3T3 (mouse fibroblasts) and CAL-72 (human osteosarcoma cells) cell lines. The first cell line was used as a model of normal cells and the second one as a model of cancer cells as dendrimers are mostly being studied as drug delivery vehicles for cancer-related applications. A metabolic activity assay (the resazurin reduction assay) was used to assess cell viability, and the results were obtained after 48 h in culture for different dendrimer concentrations as shown in Fig. 9 (the results are expressed as a percentage of the metabolic activity of the control, that is, cells that were not exposed to dendrimers). Our results reveal that the viability of NIH 3T3 cells decreased when exposed to pristine amine terminated PAMAM dendrimers, especially for the higher generations at higher concentrations, which is consistent with the results reported in the literature.[4,10] Similar results were also obtained with the CAL-72 cell line. However, the APS-treated PAMAM dendrimers were much less toxic for both cell lines, especially in the cases of G3 and G4 dendrimer generations, as can be concluded from the analysis of the IC50 values presented in Table 2. These results suggest that the synthesized APS-PAMAM dendrimers could be potentially used for biomedical applications with advantage over the pristine PAMAM dendrimers since they are less cytotoxic and do not compromise the cell internalization and imaging.

Hemotoxicity evaluation

In order to be used as bionanomaterials that need to be administered intravenously, dendrimers should be compatible with blood, namely by not causing the lysis of red cells.

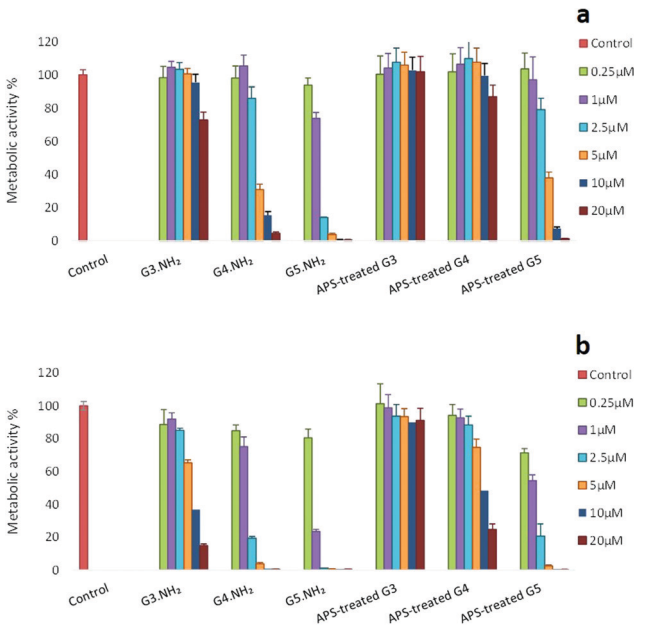

Fig. 9 Cytotoxicity of pristine and APS-treated PAMAM dendrimers after 48 h of incubation using (a) NIH 3T3 and (b) CAL-72 cell lines. The results are expressed as the mean ± SD of three independent experiments with three replicates each.

Table 2 IC_{50} values for G3, G4, and G5 pristine and APS-treated PAMAM dendrimers. For IC50 determination, experiments were performed in the 0–100 μM range

	$IC_{50} \pm SD$ (μM)	
	NIH 3T3 cells	CAL-72 cells
$G3{\cdot}NH_2$	59 ± 5	7.7 ± 0.5
$G4{\cdot}NH_2$	4.1 ± 0.2	1.7 ± 0.1
$G5{\cdot}NH_2$	1.6 ± 0.1	0.6 ± 0.1
APS-treated G3	>100	>100
APS-treated G4	64 ± 6	9.7 ± 0.7
APS-treated G5	4.3 ± 0.1	1.1 ± 0.2

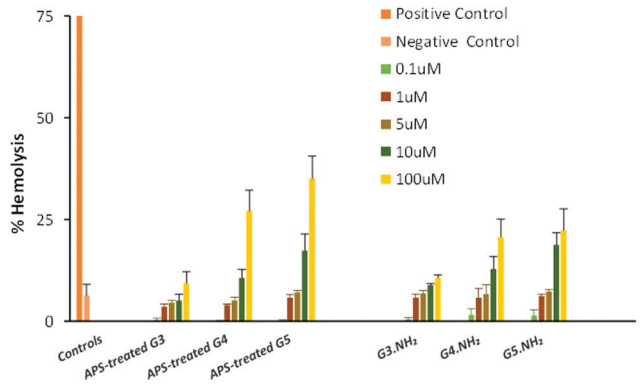

Fig. 10 Percentage of hemolysis caused by pristine and APS-treated PAMAM dendrimers at different concentrations after 3 h of incubation at 37 °C. Results are expressed as mean ± SD of three independent experiments with 3 replicates of each.

Hemolysis was then assessed for APS-treated dendrimers and compared with the results for pristine dendrimers (Fig. 10). As expected, the results showed that hemolysis increased with the concentration. However, for a concentration of 5 μM or lower, hemoglobin release was always inferior to 10% in both cases and not significantly different from the negative control. In fact, the APS-treated PAMAM dendrimers seem to be slightly less hemotoxic at lower concentrations (0.1 and 1 μM) than the pristine PAMAM dendrimers. In summary, one can consider the APS-treated dendrimers as compatible with blood in what concerns their hemolysis behaviour.

Visualization of APS-treated PAMAM dendrimers inside cells

A human bone osteosarcoma epithelial cell line (U2OS), known by being easily transfectable, was used to evaluate the possibility of detecting APS-treated PAMAM dendrimers inside cells, that is, to use them as bionanomaterials with traceability capability. G4 APS-treated PAMAM dendrimers were selected for use in these proof-of-concept assays since, compared to the other dendrimers, they present higher fluorescence emission intensity in the pH range of interest (see Fig. 5). It can be seen from Fig. 11 that these dendrimers were able to be endocytosed by cells and can be detected intracellularly as small fluorescent spots. Importantly, they seem to be present inside cellular vesicles that reside in the cytoplasm. Most probably, they are

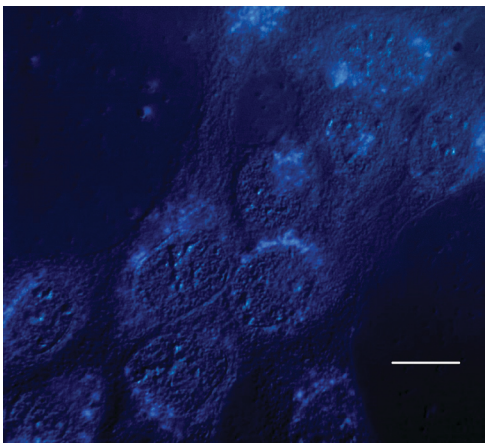

Fig. 11 Fluorescence microscopy image of U2OS cells incubated with generation 4 APS-treated PAMAM dendrimers for 24 hours (dendrimers were at a concentration of 2 μM). Scale bar = 10 μm.

emitting from acidic vesicles (like the lysosomes or endolysosomes) since, as seen before, their fluorescence emission is higher for acidic pH values. Although further experiments are needed to confirm the localization of APS-treated dendrimers inside cells, we anticipate that possibly they could be used as fluorescent markers for acidic vesicle staining.

Conclusions

The spectroscopic behaviour of different generations (G3, G4, and G5) of PAMAM dendrimers was evaluated before and after oxidation with ammonium persulfate. The APS treatment clearly resulted in the protonation of the interior of the dendrimer and in an enhancement of their intrinsic fluorescence properties. Globally, the results showed that there are at least two types of emitting electron-rich hetero-atomic subluminophores (HASLs) confined within the dendrimer scaffold that have overlapped emission bands. According to our findings and after analysing the data from the literature, we believe that these two HASLs correspond to imidic acid moieties (amide tautomers) and tertiary ammonium groups formed along with the APS treatment. In solution, fluorescence intensity was dependent not only on the pH and on the number of HASLs in the dendrimer scaffold (that is, on dendrimer generation), but also on the rigidification suffered by the dendrimer due to the acidic environment (at a low pH, APS-treated G4 was indeed the most emissive species). Moreover, photoluminescence studies with lyophilized samples confirmed the coexistence of more than one type of HASLs emitting in the dendrimer structure. The APS treatment affected these HASLs to a different extent. In accordance with the observed order of fluorescence intensity, time-resolved fluorescence experiments always showed higher average lifetimes of HASLs for APS-treated dendrimers compared to pristine ones. Interestingly, for pristine dendrimers, average lifetimes were much higher in the lyophilized samples than those in solution, which is evidence of aggregation-induced emission.

In contrast, the fraction and lifetimes of HASLs in APS-treated dendrimers were similar in solution and in the lyophilized form, probably because these dendrimers are protonated and cannot approach each other so easily due to the repulsion forces that are established. Importantly, the highly emissive APS-treated dendrimers presented lower cytotoxicity and hemotoxicity than pristine dendrimers, and were also detectable inside cells *via* fluorescence microscopy. The quantum yield, an important parameter in this type of microscopy, was high, especially for G3 and G4 APS-treated PAMAM dendrimers (75% and 63%, respectively).

To conclude, the easy preparation of these dendrimers, together with their fluorescence and biological properties, may promote their use in more widespread applications as bionanomaterials when compared to traditional PAMAM dendrimers.

Conflicts of interest

There are no conflicts to declare.

Acknowledgements

The authors acknowledge the support of FCT-Fundação para a Ciência e a Tecnologia (Base Fund UIDB/00674/2020 and Programmatic Fund UIDP/00674/2020, Portuguese Government Funds) and ARDITI-Agência Regional para o Desenvolvimento da Investigação Tecnologia e Inovação through the project M1420-01-0145-FEDER-000005-CQM^{+} (Madeira 14–20 Program) and a PhD grant (Ref. M1420-09-5369-FSE-000001) (C. C.). This work was also partially funded by Ministerio de Economía, Industria y Competitividad, Spain (Agencia Estatal de Investigación, AEI) and European Union-FEDER (MAT2016-79866-R, PID2019-107335RA-I00, PID2019-110430GB-C21). The support of the Hospital Dr Nélio Mendonça hematology service is also highly appreciated. The authors also wish to thank Dr R. Freire (Unidad de Investigación, Hospital Universitario de Canarias, Spain) for assistance in the experiments related to the visualization of dendrimers inside cells. Special acknowledgements are due to the Núcleo Regional da Madeira da Liga Portuguesa Contra o Cancro (NRM-LPCC) for the support given during the early phase of this research work through an internship granted to C. C. to start this research at CQM. The authors would also like to express their thanks to Dr Énio Freitas for the cover artwork that illustrates this article at this JMCB issue.

References

1 S. Mignani, J. Rodrigues, H. Tomás, R. Roy, X. Shi and J.-P. Majoral, Bench-to-bedside translation of dendrimers: Reality or utopia? A concise analysis, *Adv. Drug Delivery Rev.*, 2018, **136–137**, 73–81, DOI: 10.1016/j.addr.2017.11.007.

2 P. Kesharwani, K. Jain and N. K. Jain, Dendrimer as nanocarrier for drug delivery, *Prog. Polym. Sci.*, 2014, **39**, 268–307, DOI: 10.1016/j.progpolymsci.2013.07.005.

3 H. J. Hsu, J. Bugno, S. R. Lee and S. Hong, Dendrimer-based nanocarriers: a versatile platform for drug delivery, *Wiley Interdiscip. Rev.: Nanomed. Nanobiotechnol.*, 2017, **9**, e1409, DOI: 10.1002/wnan.1409.

4 M. Gonçalves, D. Maciel, D. Capelo, S. Xiao, W. Sun, X. Shi, J. Rodrigues, H. Tomás and Y. Li, Dendrimer-Assisted Formation of Fluorescent Nanogels for Drug Delivery and Intracellular Imaging, *Biomacromolecules*, 2014, **15**, 492–499, DOI: 10.1021/bm401400r.

5 S. Mignani, J. Rodrigues, H. Tomás, M. Zablocka, X. Shi, A.-M. Caminade and J.-P. Majoral, Dendrimers in combination with natural products and analogues as anti-cancer agents, *Chem. Soc. Rev.*, 2018, **47**, 514–532, DOI: 10.1039/c7cs00550d.

6 V. Leiro, J. Garcia, H. Tomás and A. P. Pêgo, The Present and the Future of Degradable Dendrimers and Derivatives in Theranostics, *Bioconjugate Chem.*, 2015, **26**, 1182–1197, DOI: 10.1021/bc5006224.

7 P. Trzepinski and B. Klajnert-Maculewicz, Dendrimers for fluorescence-based bioimaging, *J. Chem. Technol. Biotechnol.*, 2017, **92**, 1157–1166, DOI: 10.1002/jctb.5216.

8 S. P. Mukherjee, M. Davoren and H. J. Byrne, Toxicology *in vitro in vitro* mammalian cytotoxicological study of PAMAM dendrimers – towards quantitative structure activity relationships, *Toxicol. In Vitro*, 2010, **24**, 169–177, DOI: 10.1016/j.tiv.2009.09.014.

9 F. Abedi-Gaballu, G. Dehghan, M. Ghaffari, R. Yekta, S. Abbaspour-Ravasjani, B. Baradaran, J. E. N. Dolatabadi and M. R. Hamblin, PAMAM dendrimers as efficient drug and gene delivery nanosystems for cancer therapy, *Appl. Mater. Today*, 2018, **12**, 177–190, DOI: 10.1016/j.apmt.2018.05.002.

10 A. Janaszewska, J. Lazniewska, P. Trzepiński, M. Marcinkowska and B. Klajnert-Maculewicz, Cytotoxicity of dendrimers, *Biomolecules*, 2019, **9**, 1–23, DOI: 10.3390/biom9080330.

11 R. Duncan and L. Izzo, Dendrimer biocompatibility and toxicity, *Adv. Drug Delivery Rev.*, 2005, **57**, 2215–2237, DOI: 10.1016/j.addr.2005.09.019.

12 G. Wang, L. Fu, A. Walker, X. Chen, D. B. Lovejoy, M. Hao, A. Lee, R. Chung, H. Rizos, M. Irvine, M. Zheng, X. Liu, Y. Lu and B. Shi, Label-Free fluorescent poly(amidoamine) dendrimer for traceable and controlled drug delivery, *Biomacromolecules*, 2019, **20**, 2148–2158, DOI: 10.1021/acs.biomac.9b00494.

13 C. A. Dougherty, S. Vaidyanathan, B. G. Orr and M. M. Banaszak Holl, Fluorophore: dendrimer ratio impacts cellular uptake and intracellular fluorescence lifetime, *Bioconjugate Chem.*, 2015, **26**, 304–315, DOI: 10.1021/bc5005735.

14 M. Scutaru, M. Krüger, M. Wenzel, J. Richter and R. Gust, *Bioconjugate Chem.*, 2010, **21**, 2222–2226, DOI: 10.1021/bc1001906.

15 D. Wang and T. Imae, Fluorescence emission from dendrimers and its pH dependence, *J. Am. Chem. Soc.*, 2004, **126**, 13204–13205, DOI: 10.1021/ja0454992.

16 W. I. Lee, Y. Bae and A. J. Bard, Strong blue photoluminescence and ECL from OH-terminated PAMAM dendrimers in

the absence of gold nanoparticles, *J. Am. Chem. Soc.*, 2004, **126**, 8358–8359, DOI: 10.1021/ja0475914.

17 C. C. Chu and T. Imae, Fluorescence investigations of oxygen-doped simple amine compared with fluorescent PAMAM dendrimer, *Macromol. Rapid Commun.*, 2009, **30**, 89–93, DOI: 10.1002/marc.200800571.

18 A. Janaszewska, M. Studzian, J. F. Petersen, M. Ficker, V. Paolucci, J. B. Christensen, D. A. Tomalia and B. Klajnert-Maculewicz, Modified PAMAM dendrimer with 4-carbomethoxypyrrolidone surface groups-its uptake, efflux, and location in a cell, *Colloids Surf., B*, 2017, **159**, 211–216, DOI: 10.1016/j.colsurfb.2017.07.052.

19 C. L. Larson and S. A. Tucker, Intrinsic fluorescence of carboxylate-terminated polyamido amine dendrimers, *Appl. Spectrosc.*, 2001, **55**, 679–683, DOI: 10.1366/0003702011952596.

20 D. A. Tomalia, B. Klajnert-Maculewicz, K. A.-M. Johnson, H. F. Brinkman, A. Janaszewska and D. M. Hedstrand, Non-traditional intrinsic luminescence: inexplicable blue fluorescence observed for dendrimers, macromolecules and small molecular structures lacking traditional/conventional luminophores, *Prog. Polym. Sci.*, 2019, **90**, 35–117, DOI: 10.1016/j.progpolymsci.2018.09.004.

21 W. Z. Yuan and Y. Zhang, Nonconventional macromolecular luminogens with aggregation-induced emission Characteristics, *J. Polym. Sci., Part A: Polym. Chem.*, 2017, **55**, 560–574, DOI: 10.1002/pola.28420.

22 D. Wang, T. Imae and M. Miki, Fluorescence emission from PAMAM and PPI dendrimers, *J. Colloid Interface Sci.*, 2007, **306**, 222–227, DOI: 10.1016/j.jcis.2006.10.025.

23 G. Saravanan and H. Abe, Influence of pH on dendritic structure of strongly fluorescent persulfate-treated poly(amidoamine) dendrimer, *J. Photochem. Photobiol., A*, 2011, **224**, 102–109, DOI: 10.1016/j.jphotochem.2011.09.012.

24 Y. J. Tsai, C. C. Hu, C. C. Chu and T. Imae, Intrinsically fluorescent PAMAM dendrimer as gene carrier and nanoprobe for nucleic acids delivery: bioimaging and transfection study, *Biomacromolecules*, 2011, **12**, 4283–4290, DOI: 10.1021/bm201196p.

25 D. Wang and T. Imae, Morphological Dependence of Fluorescence Emitted from PbS/PAMAM Dendrimer Nanocomposite, *Chem. Lett.*, 2005, **34**, 640–641, DOI: 10.1246/cl.2005.640.

26 O. Yemul and T. Imae, Synthesis and characterization of poly(ethyleneimine) dendrimers, *Colloid Polym. Sci.*, 2008, **286**, 747–752, DOI: 10.1007/s00396-007-1830-6.

27 M. Gouveia, J. Figueira, M. G. Jardim, R. Castro, H. Tomás, K. Rissanen and J. Rodrigues, Poly(alkylidenimine)-Dendrimers Functionalizedwith the organometallic moiety $[Ru(\eta^5\text{-}C_5H_5)(PPh_3)_2]^+$ as promising drugs against cisplatin-resistant cancer cells and human mesenchymal stem cells, *Molecules*, 2018, **23**, 1–17, DOI: 10.3390/molecules23061471.

28 D. Maciel, C. Guerrero-Beltrán, R. Ceña-Diez, H. Tomás, M. Á. Muñoz-fernández and J. Rodrigues, New anionic poly(alkylideneamine) dendrimers as microbicide agents against HIV-1 infection, *Nanoscale*, 2019, **11**, 9679–9690, DOI: 10.1039/c9nr00303g.

29 S. Mignani, J. Rodrigues, R. Roy, X. Shi, V. Ceña, S. El Kazzouli and J.-P. Majoral, Exploration of biomedical dendrimer space based on *in vitro* physicochemical parameters: key factor analysis (Part 1), *Drug Discovery Today*, 2019, **24**, 1176–1183, DOI: 10.1016/j.drudis.2019.02.014.

30 S. Mignani, J. Rodrigues, H. Tomas, A. Caminade, R. Laurent, X. Shi and J.-P. Majoral, Recent therapeutic applications of the theranostic principle with dendrimers in oncology, *Sci. China Mater.*, 2018, **61**, 1367–1386, DOI: 10.1007/s40843-018-9244-5.

31 J. R. Lakowicz, *Princ. Fluoresc. Spectrosc.*, Springer, New York, 3rd edn, 2006,, DOI: 10.1007/978-0-387-46312-4.

32 I. B. Berlman, *Handbook of Fluorescence Spectra of Aromatic Molecules*, Academic Press, INC, London LTD, New York, 2nd edn,1971, DOI: 10.1016/B978-0-12-092656-5.X5001-1.

33 J. F. Gall, G. L. Church and R. L. Brown, Solubility of ammonium persulfate in water and in solutions of sulfuric acid and ammonium sulfate, *J. Phys. Chem.*, 1943, **47**, 645–649, DOI: 10.1021/j150432a003.

34 D. S. Deutsch, A. Siani, P. T. Fanson, H. Hirata, S. Matsumoto, C. T. Williams and M. D. Amiridis, FT-IR Investigation of the Thermal Decomposition of Poly(amidoamine) Dendrimers and Dendrimer–Metal Nanocomposites Supported on Al_2O_3 and ZrO_2, *J. Phys. Chem. C*, 2007, **111**(11), 4246–4255.

35 Y. Ji, L. X. Yang and Y. Qian, Poly-amidoamine structure characterization: amide resonance structure of imidic acid (HO–C═N) and tertiary ammonium, *RSC Adv.*, 2014, **4**, 49535–49540, DOI: 10.1039/C4RA09081K.

36 J. Kong and S. Yu, Fourier transform infrared spectroscopic analysis of protein secondary structures, *Acta Biochim. Biophys. Sin.*, 2007, **39**, 549–559, DOI: 10.1111/j.1745-7270.2007.00320.x.

37 Y. Shen, C. Li, X. Zhu, A. Xie, L. Qiu and J. Zhu, *J. Chem. Sci.*, 2007, **119**, 319–324, DOI: 10.1007/s12039-007-0043-3.

38 S. Pande and R. M. Crooks, Analysis of poly(amidoamine) dendrimer structure by UV-Vis spectroscopy, *Langmuir*, 2011, **27**, 9609–9613, DOI: 10.1021/la201882t.

39 Y. Wang, S. Niu, Z. Zhang, Y. Xie, C. Yuan, H. Wang and D. Fu, Reversible pH Manipulation of the Fluorescence Emission from Sectorial Poly(amidoamine) Dendrimers, *J. Nanosci. Nanotechnol.*, 2010, **10**, 4227–4233, DOI: 10.1166/jnn.2010.2195.

40 W. Chen, D. A. Tomalia and J. L. Thomas, Unusual pH-dependent polarity changes in PAMAM dendrimers: evidence for pH-responsive conformational changes, *Macromolecules*, 2000, **33**, 9169–9172, DOI: 10.1021/ma000791p.

41 D. I. Malyarenko, R. L. Vold and G. L. Hoatson, Solid state deuteron NMR studies of polyamidoamine dendrimer salts. 1. Structure and hydrogen bonding, *Macromolecules*, 2000, **33**, 1268–1279, DOI: 10.1021/ma000921u.

42 M. Konopka, A. Janaszewska and B. Klajnert-Maculewicz, Intrinsic Fluorescence of PAMAM Dendrimers—Quenching Studies, *Polymers*, 2018, **10**, 1–8, DOI: 10.3390/polym10050540.

43 M. Studzian, Ł. Pułaski, D. A. Tomalia and B. Klajnert-Maculewicz, Non-Traditional Intrinsic Luminescence (NTIL): Dynamic Quenching Demonstrates the Presence of

Two Distinct Fluorophore Types Associated with NTIL Behavior in Pyrrolidone-Terminated PAMAM Dendrimers, *J. Phys. Chem. C*, 2019, **123**, 18007–18016, DOI: 10.1021/acs.jpcc.9b02725.

44 J. Mei, N. L. C. Leung, R. T. K. Kwok, J. W. Y. Lam and B. Z. Tang, Aggregation-induced emission: together we shine, united we soar!, *Chem. Rev.*, 2015, **115**(21), 11718–11940, DOI: 10.1021/acs.chemrev.5b00263.